



A novel approach for latent print identification using accurate overlays to prioritize reference prints



Daniel T. Gantz^a, Donald T. Gantz^b, Mark A. Walch^a, Maria Antonia Roberts^c, JoAnn Buscaglia^{d,*}

^a The Gannon Technologies Group, 2303 Dulles Station Blvd., Suite 105, Herndon, VA, USA

^b Department of Applied Information Technology, Volgenau School of Engineering, George Mason University, 4400 University Drive, Fairfax, VA 22030, USA

^c Latent Print Support Unit, Federal Bureau of Investigation Laboratory Division, 2501 Investigation Parkway, Quantico, VA 22135, USA

^d Counterterrorism and Forensic Science Research Unit, Federal Bureau of Investigation Laboratory Division, 2501 Investigation Parkway, Quantico, VA 22135, USA

ARTICLE INFO

Article history:

Received 11 July 2014

Received in revised form 14 October 2014

Accepted 15 October 2014

Available online 24 October 2014

Keywords:

Fingerprint

Latent print

Mark

Ridge flow

ABSTRACT

A novel approach to automated fingerprint matching and scoring that produces accurate locally and nonlinearly adjusted overlays of a latent print onto each reference print in a corpus is described. The technology, which addresses challenges inherent to latent prints, provides the latent print examiner with a prioritized ranking of candidate reference prints based on the overlays of the latent onto each candidate print. In addition to supporting current latent print comparison practices, this approach can make it possible to return a greater number of AFIS candidate prints because the ranked overlays provide a substantial starting point for latent-to-reference print comparison.

To provide the image information required to create an accurate overlay of a latent print onto a reference print, “Ridge-Specific Markers” (RSMs), which correspond to short continuous segments of a ridge or furrow, are introduced. RSMs are reliably associated with any specific local section of a ridge or a furrow using the geometric information available from the image. Latent prints are commonly fragmentary, with reduced clarity and limited minutiae (i.e., ridge endings and bifurcations). Even in the absence of traditional minutiae, latent prints contain very important information in their ridges that permit automated matching using RSMs. No print orientation or information beyond the RSMs is required to generate the overlays.

This automated process is applied to the 88 good quality latent prints in the NIST Special Database (SD) 27. Nonlinear overlays of each latent were produced onto all of the 88 reference prints in the NIST SD27. With fully automated processing, the true mate reference prints were ranked in the first candidate position for 80.7% of the latents tested, and 89.8% of the true mate reference prints ranked in the top ten positions. After manual post-processing of those latents for which the true mate reference print was not ranked first, these frequencies increased to 90.9% (1st rank) and 96.6% (top ten), respectively. Because the computational process is highly parallelizable, it is feasible for this method to work with a reference corpus of several thousand prints.

Published by Elsevier Ireland Ltd.

1. Introduction

Latent prints¹ are impressions made by friction ridges found on hands and feet, typically from an unknown source. Although latent

prints can be visible to the unaided eye, they are usually made visible by the use of alternate light sources, chemicals, or powders. Detected latent prints are not always considered to be of value for identification purposes when analyzed by a latent print examiner, and can be so small that the proper orientation cannot be easily determined. Due to their fragmentary nature, latent prints often lack a core (center of pattern) or traditional minutiae such as ending ridges, bifurcations, and dots, which are used for automated and manual searching purposes. Latent prints containing a field of ridges without minutiae have been reported to be difficult to characterize and identify [1]. However, even in the absence of traditional minutiae, latent prints contain very important information in their ridges that permit the automated matching [2].

* Corresponding author. Tel.: +1 703 632 4553; fax: +1 703 632 7801.

E-mail addresses: dgantz@gannontech.com (D.T. Gantz),

dgantz@gmu.edu (D.T. Gantz), mwalch@gannontech.com (M.A. Walch),

maria.roberts@ic.fbi.gov (M.A. Roberts), joann.buscaglia@ic.fbi.gov (J. Buscaglia).

¹ The term “latent print” is the preferred term in North America for a friction ridge impression from an unknown source, and “print” is used generically for known or unknown impressions. We are using the North American terminology to maintain consistency with past and future papers by the authors, rather than the international preferred terminology of “mark” or “trace” for unknown impressions and “print” for known impressions.

If it is determined that the latent print and the reference print are “mated” (i.e., impressions from the same finger) and a match is determined, then in some sense the latent image can be overlaid onto the reference image. Even when the prints are mated, a rigid placement of the latent onto the reference image will exhibit some distortion between the two images due to the physical circumstances of the creation of each impression. Every impression will be distorted somewhat due to several factors (e.g., skin elasticity, substrate and pressure). The automated technology developed in this research adjusts for the distortion between the latent print and reference print impressions, providing a very accurate overlay of the print images. Specifically, the latent image is locally adjusted so that the overlay of the adjusted image to the reference image is a good fit. This fully automated technology reliably finds an optimal distortion adjusted overlay of the latent image onto any matching or nonmatching reference image. This automated technology, which has been incorporated into a latent print examiner workstation, will improve the efficiency of the latent print comparison workflow process by providing the examiner with an accurate overlay of the latent print to each reference print, thereby reducing the number of comparisons performed by the examiners. Further, a computational algorithm exploits the overlay technology to quantify similarity between the latent and reference images, and is used to rank the reference images according to their similarity to the latent.

2. Method development

The methods described in this section are novel approaches developed in this research. In order to demonstrate their feasibility, we have tested the developed methods using images taken from the NIST Special Database 27 [3]; details of the feasibility testing are presented in Section 3.

There are four parts to executing these novel technological and computational methods. The first part is the automated processing of the latent image and the reference images to determine the regions of the images with clearly defined ridge flow. The second part is the automated creation of an accurate warp of a latent image to either the mated or a nonmated reference image. The third part is the quantification of the accuracy of a warp and the selection of the overlay (i.e., “best” warp) between the latent print image and each reference image. The fourth part is the prioritization of the reference images according to the latent image overlays.

2.1. Automated processing of the latent image and the reference images

All print images are subjected to a sequence of automated processing steps. Processing steps include the binarization and skeletonization of the images, and the marking of quality regions in the images. Quality regions of a print are defined and high-contrast print images are created. First, the print image is rendered as a high-contrast image that captures ridge flow (with black ridges and white furrows) and masks out areas where reliable quality ridge flow is not present. This initial rendering process is common among many fingerprint matching technologies and a number of rendering utilities are available to perform this task [4]. In this paper, a proprietary algorithm that enhances the contrast of ridge flow based on phase measurements of bands of light and dark patterns while masking out areas lacking any dominant ridge flow is used.

Fig. 2 shows the automated progression from a sample reference image (a1) to a high-contrast representation of the image (a2) and to a “quality mask” (a3) that selects the regions with reliable quality ridge flow. The same fully automated process is performed for the latent as shown in Fig. 2 b1–b3.

Latent prints pose a variety of clarity issues, differing significantly from that of reference prints. Therefore, the quality results of automated processing will vary depending on the attributes of the latent, including complex backgrounds, overlapping prints, image clarity and other artifacts. Fig. 2 shows the automated processing of a latent from the image (c1) to the high-contrast image with the quality mask (c2) and a manual refinement (i.e., ridge tracing) (c3) of the original image (c1). An examiner can manually refine the clarity of the high-contrast image portion of the automated process when the result of that process is not adequate [5].

2.2. Automated creation of an accurate warp of a latent image to any reference image

Creating an overlay requires adjusting the continuum of ridges and furrows of the latent image to accurately fit the ridges and furrows within a region of the reference image. The latent image and each of the reference images are further processed: first, using the high-contrast images created previously, all ridges and furrows within the latent and the reference images are thinned to one-pixel wide skeletons based on center lines (Fig. 3). In this paper, a skeleton refers to the totality of the ridges and furrows. Next, continuous marking of the ridges and furrows is accomplished by covering all ridge and furrow skeletons with small curve segments. A short polynomial curve segment will accurately provide an approximate cover to a local small segment of a ridge or furrow skeleton. Computer graphics frequently makes use of Bezier curves for such local approximation, and we have selected cubic and higher order Bezier curves to approximate small segments of ridge and furrow skeletons. A cubic Bezier curve is defined by two end points and two interior control points; the curve can be altered by manipulating these four control points (Fig. 1). Higher order Bezier curves, which have more control points, are used as required to fit more complex curvature on the skeleton.

Bezier curves offer a way of describing ridges that is both compact and accurate. The four Bezier control points concisely represent the entire set of Cartesian plot points that would otherwise be explicitly necessary for curve representation. In this paper, a new Bezier curve segment of 70 pixels in length is started every 22 pixels along a skeleton for a latent image and every 3 pixels along a skeleton for a reference image (note that the difference in lengths is to provide finer coverage in the reference collection). The selection of curve segment length and location is based on all images being scaled to 500 pixels per inch (ppi); these parameters are configurable. This process provides a set of short Bezier curves that redundantly approximate ridge and furrow skeletons. Collectively, the short Bezier curves form a basis for tracking the continuum of the ridge and furrow skeletons; each Bezier curve marks a short continuous segment of a ridge or furrow and serves as a “Ridge-Specific Marker” (RSM). RSMs are reliably associated with any specific local section of a ridge or a furrow using the geometric information available from the image, making an RSM a new feature in the image [6,7]. Bezier curves are produced “through” skeleton intersections as well, such that all possible Bezier curves of the given length and step increment

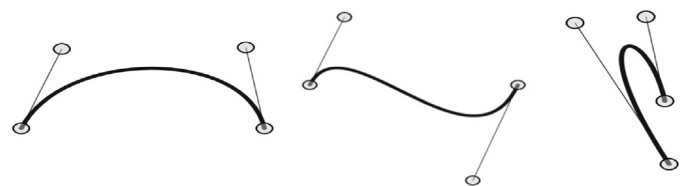


Fig. 1. Examples of cubic Bezier curves with two end and two interior control points. The curve can be altered by manipulating these four control points.

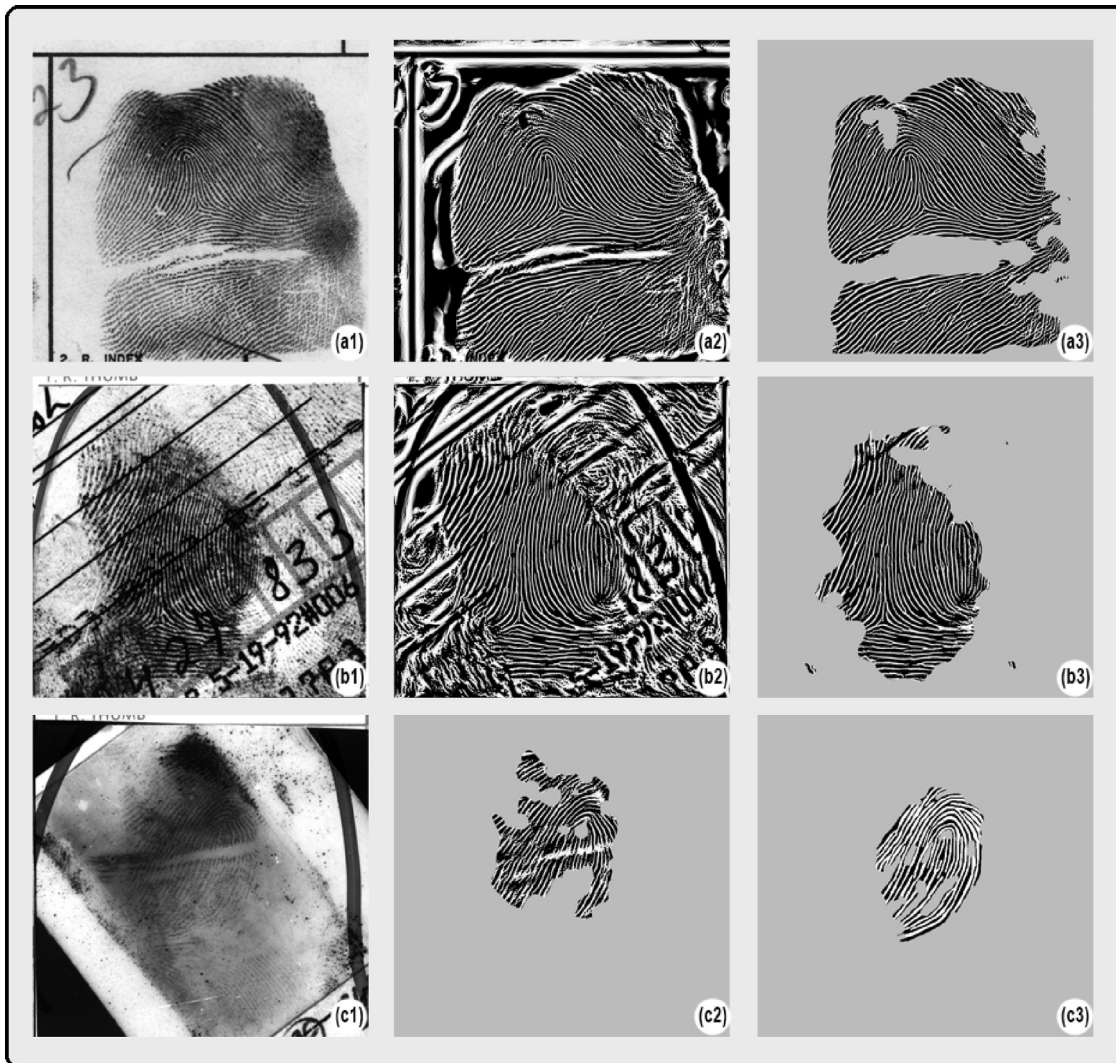


Fig. 2. (a1–a3) Show the automated progression from a sample reference image (a1) to a high-contrast representation of the image (a2) and to a quality mask (a3) that selects the regions with stable ridge flow. The same fully automated process is performed for the latent print as shown in (b1–b3). (c1–c3) Show the automated processing of a latent print from the image (c1) to the high-contrast image with the quality mask (c2) and a manual refinement (i.e., ridge tracing) (c3) of the original image (c1).

crossing through that intersection are sampled; in areas of many local intersections, the Bezier curves sampled are necessarily limited due to the combinatorial explosion of possible Bezier curves in these areas (Fig. 3).

The overlay of the latent image onto a reference image is a well-defined mathematical formula that maps the area of the latent image onto an area that contains a region of the reference image; we call this mathematical formula a “warp”. The boundaries of the latent image and the reference image are not expected to align, so the warp might place some of the transformed latent image beyond the boundaries of the reference image. It is very important to note that the warp is mathematically invertible; that is, the warp works in reverse to map the applicable region of the reference image onto the latent image. The invertibility of the warp is important because it allows segments of the skeletons of the latent image and a reference image to be compared within the latent image. In fact, the similarity of the latent image to each reference image will be assessed within the latent image, which makes it possible to compare the measured similarities among all reference images.

A warp is created by the application of a standard mathematical principle of initiating the warp on a very small part, called a seed, of

the latent image and then iteratively extending the warp across the entire latent image. The process requires many iterative steps that can be thought of as incrementally adjusting the latent image to accurately match a region of the reference image. The warp-growing algorithm is made up of logical functional libraries created in C# and refined over several years. Experimentation has verified that when the reference print is a true mate to the latent print and quality regions of the images are reasonably consistent, then an executed warp is likely to provide an accurate overlay of the latent image onto the reference image. To increase the probability that an accurate overlay of the latent image to the reference image is created, approximately 200 warps, each initiated from a different seed, are created from the latent image to a single reference image. One of these 200 warps needs to be selected to provide the overlay of the latent image onto the particular reference image: after selection of the seeds that initiate the creation of the warps, an algorithm selects one “best” warp from the latent image to the reference image as the overlay.

A seed is a single Bezier curve or a set of several Bezier curves from among the Bezier curves that cover the latent image skeleton. When a seed consists of several Bezier curves, those Bezier curves are selected within close proximity in the latent skeleton. Once a

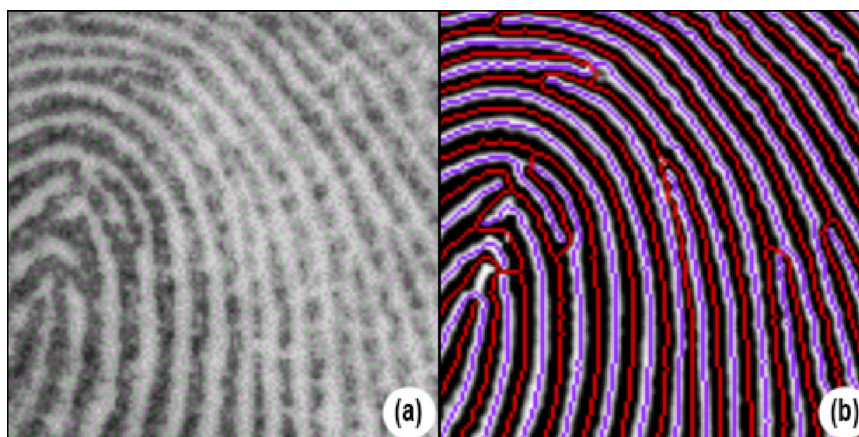


Fig. 3. Original fingerprint image (a) and example of thinned ridge and thinned furrow structure (b).

seed is selected, the first step in creating a warp is to find corresponding Bezier curves among the set of Bezier curves in the reference image skeleton on which to map the seed. This step is accomplished through the execution of multiple software functions that exploit the very geometrically informative mathematical representations for Bezier curves; these functions execute a greedy,² nonexhaustive search algorithm [8]. If the reference image is the true mate to the latent image, then it is critical that the seed in the latent image generates a warp to an accurate position in the reference image. For this reason, approximately 200 seeds are selected from the latent image; each of these seeds will lead to a warp that becomes a candidate to provide the ultimate overlay of the latent image onto a region of the reference image. The Bezier curve or curves that make up a seed are randomly selected within constraints that include comprehensive coverage of the latent image. Coverage of the latent is achieved by segmenting the region of interest in the latent into a coarse grid and sampling seeds from each grid cell, with a higher sampling frequency for those grid cells having a higher overall “quality”. Experience with the technology has shown that when the reference print is a true mate to the latent print, a significant percentage of the seeds will lead to very accurate overlays of the latent image to the correct region of the reference image.

An example of the selection of specific seeds is presented in Fig. 4. Three Bezier seed 3-tuples³ (green, orange, and red) in latent print G056L9U are depicted in a1; a2 shows the three corresponding 3-tuples of Bezier curves from seeds mapped onto the true mate reference print. The green 3-tuple in a2 is the correct placement for the green 3-tuple in a1, and the orange 3-tuple in a2 is one ridge off from the correct placement for the orange 3-tuple in a1. The red 3-tuple in a2 is an incorrect placement for the red 3-tuple in a1. Fig. 4a3 and a4 shows the placements for the green, orange, and red latent Bezier seed 3-tuples from a1 in two false (i.e., nonmated) reference prints B110T6U and B137T6U.

The mapping of the seed into the reference image induces a mapping of all of the landmark points in the latent image onto the reference image. Landmark points are the vertices of a very fine rectangular grid pattern (i.e., a mesh) that covers the latent image. Following a set of logic rules, the warp is created by adding another latent image Bezier curve iteratively to the seed; this Bezier curve is associated with a Bezier curve in the reference image and the warp is recalculated, resulting in a new induced mapping of all of the latent image landmark points onto the reference image. The

mapping of the latent image landmark points to the reference image defines the adjustments that the warp is making to the latent image so that it accurately fits a region in the reference image. The iterative steps in building the warp bring more latent image landmark points into the adjustment; the iterative addition of Bezier curves incorporates more of the latent image features, increasing the availability of features for matching and, therefore, increasing the accuracy of the warp and the likelihood of finding the true mate reference image. The iterations continue until all latent image landmark points are within the region of the aggregated Bezier curves in the latent image and therefore contribute to the adjustments. The final latent image adjustments are determined by the landmark point adjustments, and the adjustment to points in between the landmark points are interpolated from the adjusted landmark points. When the latent image is adjusted in this way by a warp to fit into a region of the reference image, the rectangular mesh covering the latent image becomes a locally stretched or squeezed mesh.

Fig. 4 shows the initial warp (b2) to the true mate reference print G056T9U for a “correct seed”. In Fig. 4, the red overlay image represents the initial warp of the latent image thinned furrow centerlines onto the reference print. The enlargement in b1 shows that the warp in the regions that are distant from the seed is not accurate due to the nonlinear distortions across both the latent and the reference image; the nonlinear warp is then iteratively refined. In Fig. 4, c2 shows the final refined warp for a “correct” seed; the enlargement in c1 shows that the warp in the regions that are distant from the seed is now accurate. The initial warps to the true mate reference print for two “incorrect” seeds are shown in b3 and b4, and the final refined warps to the true mate reference print for the two “incorrect” seeds are shown in c3 and c4.

2.3. Accuracy quantification and the selection of the optimal warp as the overlay

The accuracy of a warp is quantified at the level of single pixels within the skeletonized latent image. A given pixel in the latent skeleton is contained in multiple short Bezier curves. The basis for defining the pixel level quantification is the unique pairing of a skeletonized reference image short Bezier curve to each Bezier curve within the skeletonized latent image. This pairing is executed using the inversion of the warp, which maps the reference image target region back to the latent image. A best match to each skeletonized latent image Bezier curve is selected from among all inverted skeletonized reference image short Bezier curves; the matching criterion for Bezier curves is a distance measure for the similarity of Bezier curves. This distance measure

² “Greedy algorithms build up a solution piece by piece, always choosing the next piece that offers the most obvious and immediate benefit.” [8].

³ An n -tuple is an ordered set of n items. Here, each item is a Bezier curve.

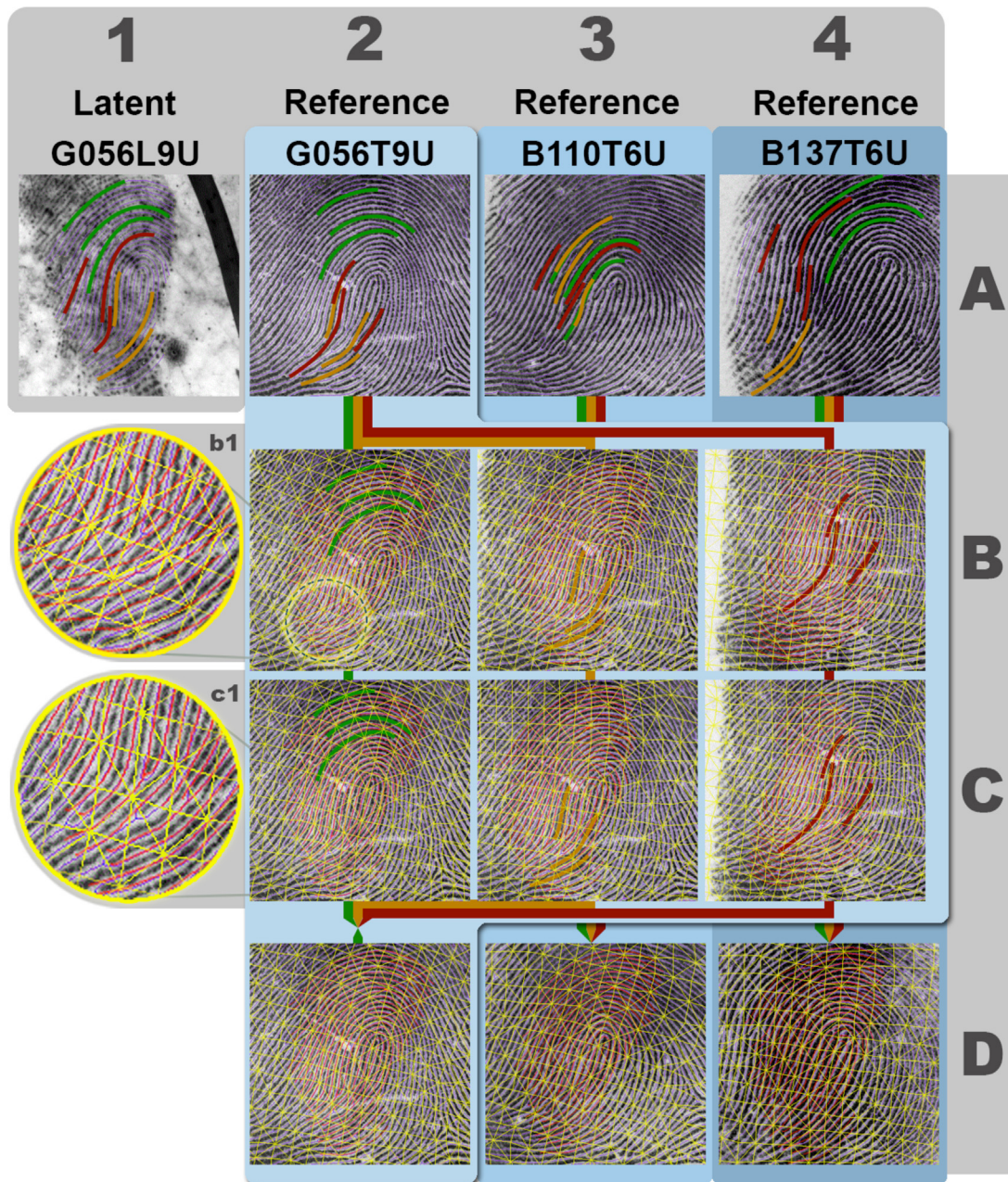


Fig. 4. All cells in this figure are referenced as row/column. Three Bezier seed 3-tuples (green, orange, and red) in latent print G056L9U are depicted in a1; a2 shows the three corresponding 3-tuples of Bezier curves from seeds mapped onto the true mate reference print. The green 3-tuple in a2 is the correct placement for the green 3-tuple in a1, and the orange 3-tuple in a2 is one ridge off from the correct placement for the orange 3-tuple in a1. The red 3-tuple in a2 is an incorrect placement for the red 3-tuple in a1. a3 and a4 show the placements for the green, orange, and red latent Bezier seed 3-tuples from a1 in two false (i.e., nonmated) reference prints B110T6U and B137T6U. In rows b, c and d, the red overlay image represents the warp of the latent image thinned furrow centerlines onto the reference print. b2 shows the initial warp to the true mate reference print G056T9U for a correctly placed seed. The enlargement in b1 shows that in the regions that are distant from the seed the warp is not accurate due to the nonlinear distortions across both the latent and the reference print. c2 shows the final refined warp to the true mate reference print G056T9U for the correctly placed seed; the enlargement in c1 shows that in the regions that are distant from the seed the overlay is now accurate. b3 and b4 show the initial warp to the true mate reference print G056T9U for two incorrectly placed seeds. c3 and c4 show the final refined warp to the true mate reference print G056T9U for the two incorrectly placed seeds. d2 provides an overlay of the latent in a1 against the true mate reference print; d3 and d4 provide two overlays against nonmate reference prints. d3 and d4 represent the “best fit” between the chosen latent and each of the two nonmate reference prints. An n -tuple is an ordered set of n items. Here, each item is a Bezier curve.

is based on the sum of square distances from sample points evenly sampled from the inverted, transformed reference image Bezier curve to closest matching points on the given latent image Bezier curve. The reference image Bezier curve whose inverted image minimizes this distance measure with a latent image Bezier curve is the one paired to the latent image Bezier curve. As mentioned above, more Bezier curves per unit length cover the reference image skeleton than the latent image skeleton; this increased

density of Bezier curves insures that one of the inverted reference image Bezier curves will closely align with a latent image Bezier curve. Fig. 5 shows a sample of thinned furrow latent image Bezier curves (a) and their closest matching thinned furrow reference image Bezier curves (b).

To quantify the accuracy of a warp, we let the symbol ω represent a pixel within the skeletonized latent image and we let w represent a warp. We define $d_w(\omega)$ as the minimum of the distance

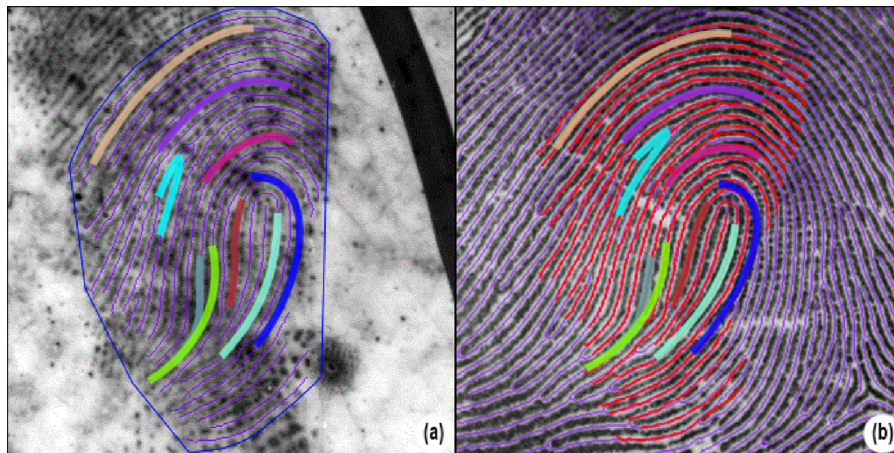


Fig. 5. An example of thinned furrow latent Bezier curves (a) and their closest matching thinned furrow reference Bezier curves (b) for a sample warp to the true mate reference print.

measures between all short Bezier curves containing the skeletonized latent image pixel ω and the warp inverted paired short Bezier curves from the skeleton of the reference image. At the latent pixel ω level, $d_w(\omega)$ quantifies the accuracy of a warp from the latent image to a reference image.

As stated previously, approximately 200 seeds are used to create separate warps of the latent image to a single reference image. A best warp has to be selected from among the many warps to become the ultimate overlay of the latent image to the reference image. An algorithm uses the pixel-level quantification of the accuracy of a warp to determine which warp is the most accurate overall. The algorithm computes pixel-level pairwise comparisons (actually competitions) between warps. The pairwise comparison score between two warps w_i and w_j at the latent pixel ω is $\log(d_i(\omega)/d_j(\omega))$, the logarithm of the ratio of the distance measures $d_i(\omega)$ and $d_j(\omega)$ for warps w_i and w_j , respectively, as defined above. If the ratio $d_i(\omega)/d_j(\omega)$ is less than one (i.e., $d_i(\omega)$ is smaller than $d_j(\omega)$), then the logarithm is negative; otherwise, the logarithm is non-negative. Thus, warps w_i and w_j are competing to have the smaller of the distance measures. We define the competitive score between w_i and w_j at the latent skeleton pixel ω as

$$S_{i,j} = -\log \frac{d_i(\omega)}{d_j(\omega)},$$

which is positive if w_i wins the competition. Note that $S_{j,i}(\omega) = -S_{i,j}(\omega)$. We modify $S_{i,j}(\omega)$ by setting $S_{i,j}(\omega) = 0$ when $S_{i,j}(\omega)$ is negative; we use this modification to focus on a positive reward to the competition winner.

For fixed warp w_i and latent skeleton pixel ω , we define $R_i(\omega)$ as the sum (over other warps w_j) of the (modified) $S_{i,j}(\omega)$ scores. Similarly, for fixed warp w_j and pixel ω , we define $C_j(\omega)$ as the sum (over other warps w_i) of the (modified) $S_{j,i}(\omega)$ scores. $R_i(\omega)$ is the total of winning scores for warp w_i in competitions with all other warps w_j ; $C_j(\omega)$ is the total of winning scores for all other warps w_j in competitions with the warp w_i . For each warp w_i and latent skeleton pixel ω , we define

$$S_i(\omega) = \log \frac{R_i(\omega) + 0.5}{C_i(\omega) + 0.5}.$$

Adding 0.5 to each of $R_i(\omega)$ and $C_i(\omega)$ assures that the logarithm of the ratio is computable. $S_i(\omega)$ is then the score that warp i takes away from the competition with all other warps at the latent skeleton pixel ω .

This approach carries out the competitive scoring among all pairs of warps based on accuracy at the skeletonized latent image pixel level. In order to rank the warps according to the relative fit of the latent image overlay to the reference image, it suffices to take the sum over all latent pixels ω of $S_i(\omega)$. The best warp has the largest sum and is the one selected to provide the overlay of the latent image to the particular reference image.

Fig. 4d shows three examples of the best warp to three reference images: d2 provides an overlay of the latent in a1 against the true mate reference print; d3 and d4 provide two overlays against nonmate reference prints, and these overlays represent the “best fit” between the chosen latent and each of the two nonmate reference prints.

2.4. Prioritization of the reference images according to the latent image overlays

Once an optimal warp that provides the overlay between the latent image and each reference image is obtained, the overlays are compared for accuracy and the reference images are scored for final ranking. The process for ranking the overlays of the latent to multiple reference images is completely analogous to that for selecting the optimal warp from a latent to a single reference image. The scoring algorithm for this process, which was described in detail above, is therefore applied to scoring and ranking the overlays to the set of candidate reference images. Once again, the scoring is pairwise between warps to reference images at the latent image pixel level, based on those latent image pixels that are mapped to reference images by both warps. Recall that a warp can map some pixels outside of the region of Bezier curves in the reference image. For each pixel in the skeletonized latent image, pairwise comparisons among reference images are computed based on the physical agreement of the pixel's best latent–reference pairs of Bezier curves as measured in latent space. The final scores for overlay warps to reference images are the sums of the pixel level scores and provide a ranking of the reference images according to the relative fit of the latent image overlays to the reference images. The candidate reference image that has the largest summed score is ranked first and the most likely match to the latent image.

Scoring of the accuracy of the overlays is latent image pixel-based. When an overlay is highly accurate, the true mate reference print should accumulate good scores with more consistency than other reference prints, resulting in the true mate reference print ranking close to the top of the candidate list. In this sense, the

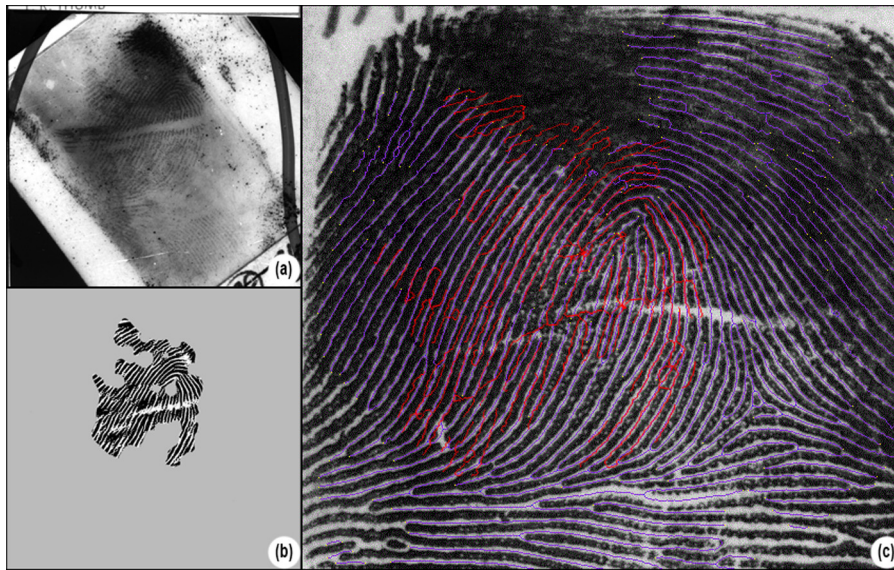


Fig. 6. With fully automated processing of the latent, the latent image (a) and high-contrast, masked image (b), plus overlay (c) to the true mate reference print for the latent G035L6U from the NIST SD27 good quality database. The overlay score for the true mate reference print is first among the 88 candidate prints.

ranking power in the ultimate score is inherently dependent on the quantity and quality of latent image pixels in relation to the true mate reference print.

3. Results and discussion

In order to test the performance of the developed methods, a feasibility study was performed using images from the NIST SD27 database. As a public dataset, the NIST SD27 database is beneficial for benchmark testing. However, the NIST SD27 images contain background, which poses an image-processing problem (i.e., separating the print from the background). Because the focus of our method is latent-to-reference matching, we selected the “good” image dataset, for which image processing issues were not a major factor.

3.1. Examples using latent prints from NIST SD27

Using fully automated processing of the latents, examples of the overlays of latents to their true mate reference prints based on the best warps are presented in Figs. 6–8.

Fig. 6 repeats both the image (a) and the high-contrast, masked image (b) for the latent G035L6U shown in Fig. 2c1, and presents the best warp of the latent onto the true mate reference print (c). This overlay is very accurate and the score ranks the true mate reference print first among the 88 reference prints.

Fig. 7 presents both the image (a) and the high-contrast, masked image (b1) for the latent G027L6U. Fig. 7c1 presents the best warp of the latent onto the true mate reference print. The overlay in c1 is not sufficiently accurate to score well; the quality of the latent in this case, due to the artifacts in the background, created a poor high-contrast image for the latent. The overlay score for the true

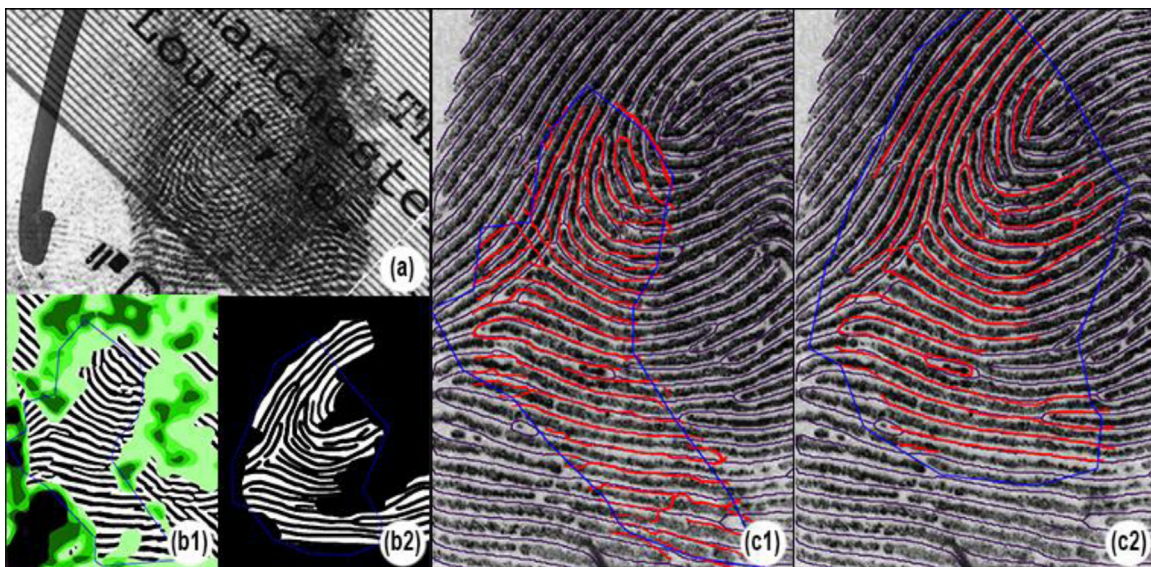


Fig. 7. With fully automated processing of the latent, the latent image (a) and high-contrast, masked image (b1), plus overlay (c1) to the true mate reference print for the latent G027L6U from the NIST SD27 good quality database, results in an overlay score for the true mate reference print that ranks it 31st among the 88 prints in the reference database. With manual refinement (i.e., ridge tracing) of the latent (b2), leading to the overlay (c2) to the true mate reference print, the overlay score for the true mate reference print makes it top ranked among the 88 candidate prints.

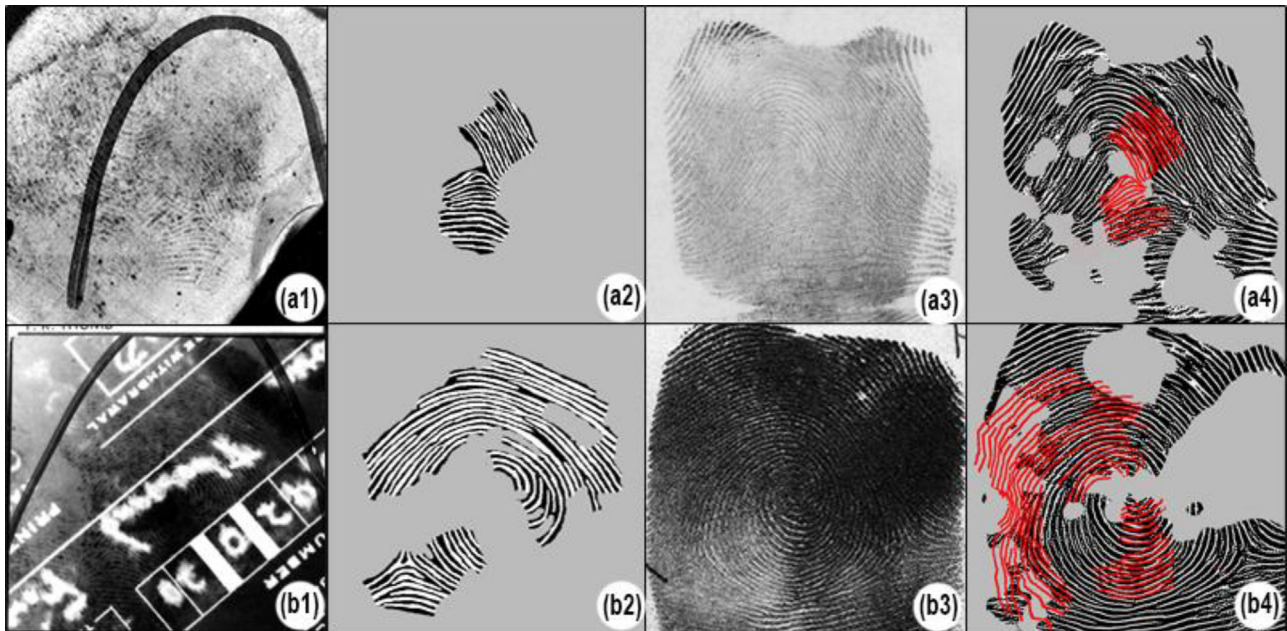


Fig. 8. Two latent print examples (G005L8U and G060L1U from the NIST SD27 good quality database) with fully automated processing of the latent illustrate the problems that arise when the true mate reference print has poor clarity in a significant corresponding area of the latent. For these two examples, respectively, the latent images (a1, b1), the high-contrast, masked image (a2, b2) of the latent prints, the true mate reference print (a3, b3) and the best warp of the latent onto the quality masked true mate reference print (a4, b4).

mate reference print ranks it 31st among the 88 reference prints. This is an instance where the characteristics of the high-contrast image indicate that it can be refined through post-processing by an examiner; Fig. 7b2 presents the results of such a manual refinement (i.e., ridge tracing) of the ridge lines and quality mask of the latent high-contrast image. For manual refinement after the fully automated processing of the latent, Fig. 7c2 presents the best warp of the latent onto the true mate reference print. The overlay is very accurate, and the overlay score for the true mate reference print now ranks it first among the 88 reference prints.

There is an imposed limit to the overlay information available when the intersection of clarity regions between the latent and the reference print do not completely correspond. The two examples (G005L8U and G060L1U) in Fig. 8 illustrate the problems that arise when the true mate reference print has poor clarity in a significant corresponding area of the latent. Both examples show the latent images (a1, b1), the high-contrast, masked images (a2, b2) of the latent prints, the true mate reference prints (a3, b3) and the best warps of the latent onto the quality masked true mate reference prints (a4, b4).

In both examples, the overlay is not uniformly accurate; for G005L8U, accuracy is not good in the lower region of the overlay that coincides with a masked-out portion of the true mate reference print. Due to lack of clarity in the corresponding areas between the latent and true mate reference print, the score is diminished, resulting in the true mate ranking fourth (out of 88) in the candidate list. For G060L1U, Fig. 8b4 depicts a very fragmented quality mask; the absence of corresponding area on the reference print causes the best warp to be incorrect. The incorrect warp leads to the true mate ranking last (i.e., 88th) in the candidate list. Solutions to these problems are currently under development, including the use of several fused individual fragments both from the latent and reference images.

3.2. Scoring

The fully automated processing of many of the 88 NIST SD27 good quality latent prints provided overlays of the latent to the

true mate reference print that scored in top rank among the entire corpus of 88 reference prints; latent print G035L6U (Fig. 6) is a representative example. Table 1 provides the overall rankings of the true mate reference prints for all latents tested using a fully automated approach. For the fully automated approach, the only user interaction involves selecting with a polygon, or multiple polygons, the search area on the latent image. The area selected would encompass only friction ridge detail of interest, thus eliminating other superfluous prints or print-like marks that may be in the image. For the 88 latent prints tested using the fully automated approach, 80.7% of the true mate reference prints were ranked in the top candidate position, 9.1% were ranked in positions 2–4, and the remaining 10.2% of the latents produced candidates ranked beyond the first 10 positions.

For those latent images whose true mate reference prints were not ranked in the top position using fully automated processing, Table 1 provides rankings using manual post-processing (e.g., ridge tracing). As seen in Table 1, with the incorporation of some additional manual post-processing, it is possible to improve the fully automated rankings of the true mate reference prints; latent print G027L6U (Fig. 7) is an example of improving the rank position of the true mate reference print from 31st to the top rank with

Table 1

Frequencies of rankings by overlay scores for 88 latent “good” latent prints from NIST SD27 tested against the reference corpus of 88 using fully automated processing, followed by manual post-processing of those latents for which automated processing did not rank the true mate reference image in the top position.

Rank (out of 88)	Number of latents with listed rank	
	Fully automated processing	Manual post-processing
1	71	80
2	4	2
3	1	0
4	3	2
5–10	0	1
>10	9	3

manual post-processing. After manual post-processing, 90.9% of the true mate reference prints were in the first rank and 96.6% were in the top ten positions.

4. Conclusions

A method has been presented for creating an overlay of a latent image onto each fingerprint image in a reference corpus; this method uses only the defined RSMs to create the overlay. Traditional minutia points have not been incorporated in order to demonstrate the matching power in RSMs alone. When both the latent and the true mate reference print have corresponding good quality ridge detail, the fully automated process produces a very accurate overlay of the latent image onto the reference image. Further, in this case, the accuracy-based scoring provides a very high ranking score to the true mate reference print. When the attributes of the latent print or reference print indicate that it is required, some manual processing by an examiner may be necessary to enhance the quality of the masked, high-contrast image of the latent. Except in instances illustrated in Fig. 8 (i.e., when the true mate reference print has poor clarity in a significant overlay area of the latent), the process provides a properly placed and accurate overlay of the latent onto the true mate reference print.

This technology was originally created as a tool to help latent print examiners using AFIS to search and potentially identify latent prints, and lead to more accurate AFIS candidate lists. The technology may be useful to exploit latent prints previously determined to be of limited or no value for identification due to size, quality, or sparse minutiae. Using this approach, a larger AFIS candidate list could be returned, thereby increasing the likelihood of finding the true mate for low quality latent prints. The technology would then prioritize the AFIS larger candidate list, increasing the efficiency of the latent print examination process. The system could also be used in a closed system as a stand-alone per case scenario. Finally, because the process described herein is highly parallelizable, it is feasible for this method to work with a reference corpus of several thousand.

Acknowledgments

The authors gratefully acknowledge the contributions of Terry Green, Joseph Brown and Christopher Saunders to this research and manuscript.

This work was supported in part under a Contract Award from the Counterterrorism and Forensic Science Research Unit of the Federal Bureau of Investigation Laboratory Division. This is publication number 14-12 of the Laboratory Division of the Federal Bureau of Investigation. Names of commercial manufacturers are provided for information only and inclusion does not imply endorsement by the FBI or the U.S. Government. The views expressed are those of the authors and do not necessarily reflect the official policy or position of the FBI or the U.S. Government.

References

- [1] C. Champod, C. Lennard, P. Margot, M. Stoilovic, *Fingerprints and Other Ridge Skin Impressions*, CRC Press, Boca Raton, FL, 2004.
- [2] J. Feng, Z. Ouyang, A. Cai, Fingerprint matching using ridges, *Pattern Recognit.* 11 (2006) 2131–2140. , <http://dx.doi.org/10.1016/j.patcog.2006.05.001>.
- [3] M.D. Garriss, R.M. McCabe, NIST Special Database 27 Fingerprint Minutiae from Latent and Matching Tenprint Images, U.S. Department of Commerce, National Institute of Standards and Technology, Gaithersburg, MD, June 2000, Available at ftp://sequoyah.nist.gov/pub/nist_internal_reports/ir_6534.pdf.
- [4] R. Hastings, Ridge Enhancement in Fingerprint Images using Oriented Diffusion, IEEE Computer Society, Digital Image Computing Techniques and Applications, 2007, <http://dx.doi.org/10.1109/DICTA.2007.84> Available at http://www.csse.uwa.edu.au/~bobh/research/fingerprints/DICTA2007_bobh.pdf.
- [5] D. Maltoni, D. Maio, A.K. Jain, S. Prabhakar, *Handbook of Fingerprint Recognition*, Springer, London, England, 2009.
- [6] S.J. Taylor, E.K. Dutton, P.R. Aldrich, B.E. Dutton, Application of Spatial Statistics to Latent Print Identifications: Towards Improved Forensic Science Methodologies, Document #NCJ240590, U.S. Department of Justice, 2012 Available at <https://www.ncjrs.gov/pdffiles1/nij/grants/240590.pdf>.
- [7] V. Perumal, J. Ramaswamy, An innovative scheme for effectual fingerprint data compression using Bezier curve representations, *Int. J. Comput. Sci. Inf. Secur.* 6 (1) (2009) (ISSN 1947-5500).
- [8] S. Dasgupta, C. Papadimitriou, U. Vazirani, *Algorithms*, McGraw-Hill, New York, NY, 2008.